Balancing food and density-dependence in the spatial distribution of an interference-prone forager

Dokter, A.M.; van Loon, E.E.; Rappoldt, C.; Oosterbeek, K.; Baptist, M.J.; Bouten, W.; Ens, B.J.

DOI
10.1111/oik.04139

Publication date
2017

Document Version
Final published version

Published in
Oikos

Oikos 126: 1184–1196, 2017
doi: 10.1111/oik.04139

Subject Editor: Rob Robinson. Editor-in-Chief: Dries Bonte. Accepted 4 January 2017

Balancing food and density-dependence in the spatial distribution of an interference-prone forager

Adriaan M. Dokter, E. Emiel van Loon, Cornelis Rappoldt, Kees Oosterbeek, Martin J. Baptist, Willem Bouten and Bruno J. Ens

A. M. Dokter (a.m.dokter@uva.nl), E. E. van Loon, W. Bouten, Computational Geo-Ecology, Inst. for Biodiversity and Ecosystem Dynamics, Univ. of Amsterdam, Science Park 904, Amsterdam, the Netherlands. AMD also at: Centre for Avian Migration and Demography, Dept of Animal Ecology, Netherlands Inst. of Ecology (NIOO-KNAW), Wageningen, the Netherlands. – C. Rappoldt, Ecocurves, Haren, the Netherlands. – K. Oosterbeek and B. J. Ens, Sovon Dutch Centre for Field Ornithology, Coastal Ecology Team, Den Burg, Texel, the Netherlands. – M. J. Baptist, Wageningen University and Research, Wageningen Marine Research, Den Helder, the Netherlands.

Foraging distributions are thought to be density-dependent, because animals not only select for a high availability and quality of resources, but also avoid conspecific interference. Since these processes are confounded, their relative importance in shaping foraging distributions remains poorly understood. Here we aimed to rank the contribution of density-dependent and density-independent effects on the spatio-temporal foraging patterns of eurasian oystercatchers. In our intertidal study area, tides caused continuous variation in oystercatcher density, providing an opportunity to disentangle conspecific interference and density-independent interactions with the food landscape. Spatial distributions were quantified using high-resolution individual tracking of foraging activity and location. In a model environment that included a realistic reconstruction of both the tides and the benthic food, we tested a family of behaviour-based optimality models against these tracking data. Density-independent interactions affected spatial distributions much more strongly than conspecific interference, even in an interference-prone species like oystercatchers. Spatial distributions were governed by avoidance of bill injury costs, selection for high interference-free intake rates and a decreasing availability of benthic bivalve prey after their exposure. These density-independent interactions outweighed interference competition in terms of effect size. We suggest that the bottleneck in our mechanistic understanding of foraging distributions may be primarily the role of density-independent prey attributes unrelated to intake rates, like damage costs in the case of oystercatchers foraging on perilous prey. At a landscape scale, above the finest inter-individual distances, effects of conspecific interaction on spatial distributions may have been overemphasised.

The notion that animals are expected to distribute so as to maximise their fitness rewards is at the heart of ecological theory on optimal habitat selection. Fretwell and Lucas (1969) were the first to formalise this idea in their definition of the ideal free distribution (IFD). In this model animals are "ideal" by being able to assess their full spatial landscape of fitness rewards, as well as "free" to move between habitats without cost. In addition, animals are assumed to be identical, which under a constraint of fitness maximisation implies that all foragers achieve identical fitness rewards. In case of a standing stock of prey and in absence of mutual interference, the IFD predicts all foragers should concentrate in the single patch where the highest fitness gains can be realised (Lessells 1995, van der Meer and Ens 1997). Such behaviour is rarely observed at the landscape scale, i.e. the range of tens of metres to many square kilometers at which populations of foragers distribute within an ecosystem (Turner 1989). Because foraging processes are usually dependent on the density of conspecifics, some foragers will move to other patches to avoid mutual interference, thereby increasing the overall fitness rewards. The IFD is therefore an inherently competitive distribution, based on the key ecological concepts of fitness maximisation and density dependent regulation.

Studies have varied greatly in their assumptions on the relative importance of density-dependence as a driver of landscape-scale distributional patterns. On the one extreme, mechanistic animal distribution models have treated density dependence as the main 'repulsive force' that spreads animals over multiple habitats and patches (Bautista et al. 1995, van der Meer and Ens 1997, van Gils and Piersma 2004). Because fitness rewards associated with foraging are difficult to express in terms of future reproductive success, many authors have assumed that foraging animals maximise instantaneous intake rate as a short-term fitness proxy (Holling 1959, Sutherland 1983, Kacelnik et al. 1992). A focus of mechanistic habitat selection studies has therefore been the characterisation of functional responses (Bautista et al. 1995, van Gils et al. 2004, Duijns et al. 2015), defined as the energetic intake rate as function of prey attributes, prey

density, and, in the case of generalised functional responses, competitor density (van der Meer and Ens 1997). Because interference competition generally reduces intake rates as a result of time lost in conspecific interactions and prey lost by kleptoparasitism, spatial distributions may be strongly regulated by direct competitive interactions between individuals that affect intake rates (Sutherland 1983, Goss-Custard et al. 1995, van der Meer and Ens 1997, Folmer et al. 2012). Indeed, van der Meer and Ens (1997) showed that, at least theoretically, foraging distributions can be highly sensitive to how intake rates depend on conspecific density. Field tests of these ideas with free-living foragers in real ecosystems are however difficult, because the density of foragers is always directly confounded with the density (and quality) of the food.

On the other extreme, most phenomenological resource selection studies have neglected density-dependence altogether (reviewed by McLoughlin et al. 2010). The main reason for discarding density-dependence has been primarily computational efficiency and model simplicity, however the extent in which this simplification affects ecological inferences is unknown. To assess the relative importance of density dependence (both from a fundamental ecological and practical modelling perspective) we need to quantify the balance between density-dependent and density-independent effects on landscape-scale distributions in real ecosystems, which is the aim of this study.

Eurasian oystercatchers *Haematopus ostralegus* were used as a study species, because they are are known to be highly interference-prone (Ens and Goss-Custard 1984, Triplet et al. 1999) and have therefore become a model species for studying competitive distributions. We therefore hypothesised that density dependence by mutual interference between oystercatchers would strongly affect the landscape-scale aggregative response at our study site. Wintering oystercatchers forage primarily in intertidal areas (van de Pol et al. 2014), where patches are alternatingly exposed and flooded by the tides. The tidal movements cause a natural modulation of the foragers' density, to which density-dependent effects and density-independent effects will respond differently. Intertidal systems hereby provide an opportunity for disentangling the respective effects of density-dependent interference and density-independent predator–prey interactions.

We used high-resolution individual GPS tracking, which can quantify the dynamic distributional patterns of oystercatchers in intertidal ecosystems at high spatial detail (Bouten et al. 2013, Schwemmer et al. 2016). These tracking data not only provide information on habitat preferences, but also – important for our study – on the density of foragers: patches with a high forager density simply have a higher chance to be visited by the tracked cohort of individuals. We present a general Bayesian approach to quantify this information on density, and to rigorously compare the highly dynamic distributional patterns with model predictions from a family of density-dependent optimality models.

Many recent studies have shown that animals are not only selective for gross energetic intake rate, but consider other prey quality attributes as well, like digestibility (van Gils et al. 2005), toxicity (Oudman et al. 2014), parasite load (Hulscher 1982), specific nutrients (Graveland and Berends 1997), metabolic costs (Wood et al. 2013), or injury risks (Rutten et al. 2006). These effects change the central foraging currency of optimality models (Houston and McNamara 2014) into more complex functional forms that may be difficult to parametrise a priori (Brown and Kotler 2004). We will show how to include such parameter uncertainty into mechanistic distribution models, which is important for model comparison in order to focus on differences in biological mechanisms rather than differences in exact parametrisations that may be poorly supported by observations.

Material and methods

Study site

Our study was performed at a 50 km^2 tidal flat area called 'Balgzand', in the westernmost part of the Dutch Wadden Sea (53°N, 5°E). The site is described in detail in earlier publications (Beukema 1974, Beukema and Cadée 1997, Dekker and Beukema 2012) and in the supplemental material. Monthly counts of oystercatchers on Balgzand revealed that around 8000–15 000 individuals used this area in the winter 2011–2012 (Supplementary material section 1). Oystercatchers overwinter in the Dutch Wadden Sea mostly from Aug–Feb, when numbers are relatively constant around 120 000 individuals (Hornman et al. 2013).

GPS tracking and accelerometer data

Analyses were carried out on tracking data of 10 individual oystercatchers (eight adults and two 2-year birds). These birds were tagged in the nights of 1–2 and 2–3 August 2011 on a mudflat central in the study area (indicated by blue cross in Fig. 1), and equipped with GPS loggers (Bouten et al. 2013). The tags delivered a high resolution GPS fix every hour up to every 30 min when the battery was full and charging (typically during day-time). Following each GPS fix we took 1 s of tri-axial accelerometer data at 20 Hz (Shamoun-Baranes et al. 2012), from which we derived an activity status that indicated whether the bird was actively foraging, which shows by a higher dynamic body acceleration than when standing still or performing body care (Shamoun-Baranes et al. 2012). For distribution modelling we confined the data to a four week period (15 October–15 November 2011), which coincides with the sampling period of the benthic prey. Details on the GPS system, measurement schemes and accelerometer analysis can be found in the Supplementary material section 2.

Tidal reconstruction

The semi-diurnal tides during the study period were spatially reconstructed by linearly interpolating between three permanent tidal stations and four tidal stations calibrated on the data of water pressure loggers fixed at the surface of the mudflats (indicated by blue and green crosses in Fig. 1, Supplementary material section 3). The permanent stations provided data every 10 min, and we used the same interval

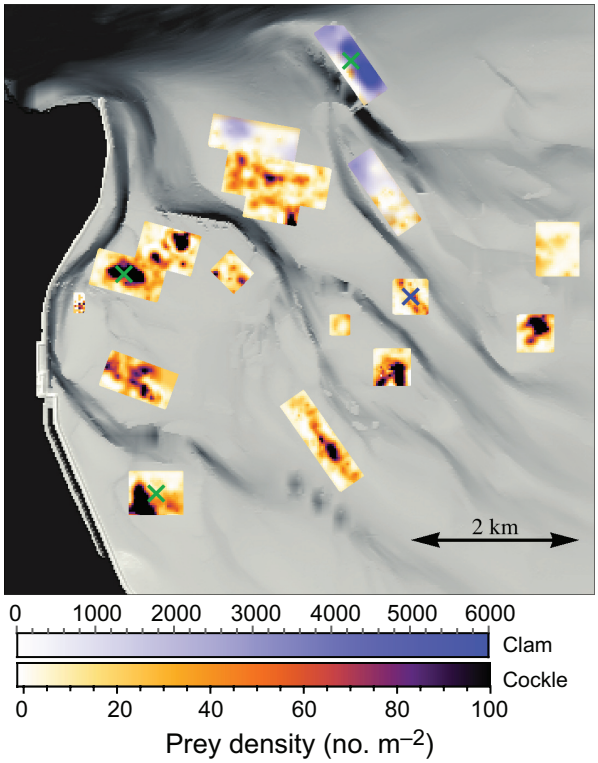

Figure 1. Density of oystercatchers' two main food resources in late October/early November 2011. Orange-red colors indicate the numerical density of cockles *Cerastoderma edule*. Blue colors indicate numerical density of razor clam *Ensis directus*. Bathymetric relief is indicated in greyscale. The green and blue crosses indicate measurement stations for tidal height. Birds were captured at the blue cross.

for the interpolations. A bathymetric map of the area was provided by Rijkswaterstaat, Ministry of Infrastructure and the Environment (cycle 5 map at 20 m resolution, (Elias and Wang 2013)). Areas were considered accessible for foraging when they were exposed or flooded by 10 cm water or less (in cages a 15 cm upper limit was observed, but water there is clearer and flatter, making 10 cm more representative of the wild, Rutten et al. 2010a).

Available prey and geospatial interpolation of survey data

A benthos survey took place in the period from 26 October 2011 to 11 November 2011. Sampling was limited to 17 rectangular grids, which included the intensively used areas by the GPS-tracked individuals, as assessed from maps of GPS fixes acquired the month preceding the study period. Also little selected habitat was included, such that the survey had a high chance of encompassing both preferred and not preferred habitat (details protocol are given in the Supplementary material section 4.2–3).

The parallel long-term monitoring program of benthos at Balgzand identified cockles *Cerastoderma edule*, American razor clams *Ensis directus* and mussels *Mytilus edulis* as available bivalve prey for oystercatchers (Supplementary material section 4.1). Mussels were not considered in our sampling program because the contours of mussel beds in which this species aggregates were known. None of our GPS-tracked individuals visited these beds, and visual observations confirmed a low attendance by oystercatchers of these beds. The full sampling program was repeated from 23 February 2012 to 20 March 2012 to assess changes in the food stock.

Spatial resolution of the surveys was chosen to match the characteristic spatial scale of the tracking data patterns observed up to the start of the sampling, which required high resolution sampling on a 50 m grid (Supplementary material section 4). Such high resolution sampling is only feasible over a limited area, therefore we restricted our sampling to 17 rectangular grids (Fig. 1). The survey included most of the intensively used areas by the GPS-tracked individuals, taking care to include also little used habitats around the intensively used areas. We found that 50.2% of the surveyed stations contained no prey, therefore both high and low quality feeding habitats were represented in the survey.

We made interpolated maps of prey biomass density and prey size using ordinary kriging (implemented in the R package gstat, Pebesma 2004), based on a single variogram per prey species for the entire study area (Supplementary material section 4) on a 25 m grid. We refer to these 25×25 m grid cells as foraging patches.

Modelling oystercatcher foraging and distribution

Despite mixed findings on the empirical succes of the IFD (Kennedy and Gray 1993, Milinski 1994, Tregenza 1995), it remains highly influential in contemporary studies of animal distributions (van Gils et al. 2006, Quaintenne et al. 2011). The IFD explains habitat selection as an emergent pattern of behaviour, and is founded in ecological theory, which is an advantage over purely phenomenological resource selection models (McLoughlin et al. 2010). We therefore use the IFD as a starting point. We start with a general roadmap of our modelling approach, followed by a detailed description of the model components.

Modelling approach

1. Goal of the modelling exercise is to rank established mechanisms for our model species in terms of their contribution to spatial foraging patterns, in particular density-dependent effects (conspecific interference) versus density-independent effects.
2. Known functional insights into the individual-level foraging process were incorporated into the spatial models as much as possible, i.e. functional responses were parametrised from the literature.
3. Other unknown (or poorly known) parameters were included as free parameters. These model parameters were estimated against the tracking data and a reconstruction of the environment (food landscape and tides), using Bayesian parameter estimation with Markov chain Monte Carlo (MCMC) methods.
4. We quantified the losses in model performance after removing model components from the full model. This we used as a metric to quantify how important those components were in describing spatial patterns.

Structure and components of the oystercatcher foraging model

We assumed animals distributed over the available patches in the system such that the fitness gain rate is maximised for all individuals. We further assumed that a group of identical foragers with average behaviour could approximate the foraging process. In this case the maximisation constraint implies that at time t all foragers realise the same gain rate c_t. For a foraging patch k containing prey items of type j we may write:

$$\begin{aligned}\text{Gain rate in k} = &\left(\overset{\text{component 1}}{\text{capture rate } f_j}\right)\times\left(\overset{\text{component 2}}{\text{Prey effect } G_j}\right)\\ &\times\left(\overset{\text{component 3}}{\text{Energy / prey item } b_j}\right)\\ &\times\left(\overset{\text{component 4}}{\text{Damage } K_j}\right)\times\left(\overset{\text{component 5}}{\text{Interference } I_j}\right)\\ &= c_t \text{ for all occupied k}\end{aligned} \quad (1)$$

Because within patches typically only a single prey type occurred in our study area, we further assumed that birds foraged only on the prey type with highest interference-free gain rate in that patch.

Model components can be removed by equating them with unity or by removing dependencies on prey type j. The common prey types in the study area were cockles *Cerastoderma edule* and spat of the American razor clam *Ensis directus*.

Component 1. Prey capture rate f

Field data on prey capture rates as a function of prey density were described with a Holling type II functional response (Holling 1959), also known as the disc equation:

$$f_j(n_{jk}, s_{jk}) = \frac{A_j n_{jk}}{1 + A_j n_{jk} h_j(s_{jk})} \quad (2)$$

with n_{jk} the numerical density and s_{jk} the size of prey type j in patch k, A_j the attack rate and h_j the handling time of the prey (not be confused with the terminology used in some resource selection studies, where functional response refers to a change in preference with overall habitat availability, Mysterud and Ims 1998, Matthiopoulos et al. 2011).

The function describing the capture rate of cockles is based on a compilation of data from ten studies (Zwarts et al. 1996), using a non-linear fit on the capture rates of Holling's disc equation with size-dependent handling time. For *Ensis directus* spat no functional response was available in the literature, therefore a functional response for oystercatchers feeding on this prey was determined from intake rate observation on this prey in the study area (see Supplemental material section 5 and Fig. A9–A10 for details).

Alternatively, we may assume that because of digestive constraints, birds perceive patches equivalent when the intake rate exceeds the digestion rate r_{digest}, as hypothesised in digestive rate models (van Gils and Piersma 2004). This behaviour is easily simulated by replacing f_j in Eq. 2 by $f_j^{digest} = \min(f_j, r_{digest} / b_j)$, with b_j the energetic content of the prey (see component 3) and r_{digest} the digestive rate for oystercatchers determined by Kersten and Visser (1996) (0.263 g wet weight min^{-1}, converted to 0.7 mg AFDW s^{-1} using a wet weight to AFDM conversion factor of 0.16 (following Zwarts et al. 1996)).

Multiplication of the capture rate with the energetic value per prey item (cf. component 3 below) gives the interference-free intake rate.

Component 2. Prey response G

Several authors have suggested capture rates may be larger at the tide line (Duijns and Piersma 2014), which would be the mechanism underlying tide line following, as observed in several wader species (Recher 1966). Birds may be more successful at capturing prey when it is still submerged, or has recently been exposed at ebb tide. In the model we therefore included an active bivalve prey, in which the prey availability changes after being exposed. The effect is therefore modelled as a multiplicative factor G_j that acts on the capture rate, given by

$$G_j(t, t_k | \tau_j, B_j) = \frac{1}{\Gamma_j}\left(1 + B_j e^{-\frac{t - t_k}{\tau_j}}\right) \quad (3)$$

Here B_j is the relative increase of the functional response in the waterline and t_k the time at which patch k got exposed (which is different for each exposing tide). The time constant τ_j determines how quickly the effect disappears after exposure. The normalisation factor Γ_j follows from the boundary condition that the capure rate including the prey effect averaged over an ordinary low tide period of duration $\bar{L}$ (within which functional responses are measured in the field) should be the same as the capture rate without the prey effect, that is

$$\int_0^{\bar{L}} G_j(t, 0 | \tau_j, B_j)\,dt / \bar{L} = 1 \overset{\text{yields}}{\rightarrow} \Gamma_j = 1 + \tau_j B_j \left(1 - e^{-\frac{\bar{L}}{\tau_j}}\right) / \bar{L} \quad (4)$$

We take $\bar{L} = 6.2$h, half the duration of an average tidal cycle. To model species-specific behaviour of the prey we may use different parameters τ_j and B_j for each prey species j, i.e. τ_{cockle} and B_{cockle} for cockles and τ_{clam} and B_{clam} for razor clams.

Component 3. Energetic value prey items b

To calculate intake rates we need to multiply the capture rate with the prey-size dependent ash-free dry mass per prey item $b_j(s_{jk})$. Following Honkoop and Beukema (1997) and Dekker and Beukema (2012), the ash-free dry mass can be written as a multiplication of a body mass index (BMI) of the prey times the cube of its average size s_{jk}:

$$b_j\left(s_{jk}\right) = \text{BMI}_j\, s_{jk}^3 \quad (5)$$

The BMI of bivalve prey is seasonally dependent and slowly decreases during winter (Honkoop and Beukema 1997). BMI values were taken from the long-term benthic survey program at our study site determined in the same season (Table 2, Supplementary material section 4.3), and kept constant for the limited period of our case study (15 October –15 November).

Component 4. Damage K

Oystercatchers have been shown to avoid foraging on perilous prey that may cause bill tip damage (Rutten et al. 2006). Cockles are a key prey species for oystercatchers, but

bill tip damage occurs easily when foraging on its larger size classes (over 40% of animals hurt their bill tip on cockles of >30 mm, Rutten et al. 2006). Since in our study year, most cockles were relatively large, inclusion of damage effects in our model was required. The other prey common in our study area, razor clam spat, has a much thinner shell, which cannot close at the top. This prey can therefore be captured and consumed without a risk of bill damage. Component 4 describes the energetic loss due to damage incurred while handling a prey item. We model the effect of damage as a perceived reduction in the energetic gains per prey item.

$$\bar{b}_j(s) = b_j(s) K_j \quad (6)$$

The cost of damage for foraging on razor clam spat is likely negligible compared to the cost of damage for foraging on cockles. We therefore set $K_{clam} = 1$ (no bill damage) and include $K_{cockle}(s) = K_{cockle}$ as a model parameter. In Appendix 1 we show that the factor K_{cockle} is related to a rate of bill damage that is proportional to prey size s, such that larger prey items inflict more damage.

Component 5. Interference competition I

We model conspecific interference competition as a multiplicative exponential term to the functional response, i.e.

$$I_j = e^{-q_j p_k} \quad (7)$$

with p_k the predator density in patch k and q_j the interference constant on prey j. We had no prior evidence that inter-specific competition played a role at our site, which was therefore not considered. We used this interference model for two reasons. First, an exponential interference effect is expected on geometrical grounds for any interference mechanism that has a characteristic length scale, such as an attack range in the case of kleptoparasitism or a disturbance distance in the case of prey depression (Rappoldt et al. 2010). In the case of oystercatchers, the interference effect in behaviour-based model simulations of kleptoparasitic behaviour was shown to be exponential, which is a major interference component in this species (Stillman et al. 2002, Rappoldt et al. 2010). Second, solutions to the IFD for this interference model are invariant to assumptions on the total number of birds N occurring in the study area, as shown in Appendix 2. This is a very useful property when the absolute number of birds that use the study area is not known exactly. To make the interference dependent on prey type we may use different parameters q for each prey species, i.e. q_{cockle} for cockles and q_{clam} for razor clam spat. According to field data (Triplet et al. 1999), experimental data (Rutten et al. 2010a, b), and an individual-based competition model (Stillman et al. 2002, Rappoldt et al. 2010), the interference constant for cockles is approximately 5–12 m^2, therefore we chose $q_{cockle} = 8$ m^2 in our null model of intake rate maximization.

Fitting behaviour-based models on tracking data

Our approach is to use the GPS-tracked individuals as spatial probes of the true population distribution. Tracked individuals provide information on population density, because, on average, patches with a high forager density will also have the highest probability of being visited by one of the GPS tracked individuals. This implicit density information can be compared with density predictions of behaviour-based models, as derived explicitly in Appendix 3.

We assumed 5000 birds were foraging in the patches, which was estimated based on the surveyed area and the total number of birds wintering in the study area (8000–15 000, Supplementary material section 1), however the performance of the models did not depend on this assumption (Appendix 2). We further assumed that the total number of birds present in the patches follows the same tidal pattern as the presence of GPS birds in the patches, as shown in Fig. 2 (bars). The number of birds N_t released in the model at time step t therefore equals 5000 multiplied by the proportion in patches corresponding to the reference tide at that time.

The vector of free model parameters β was estimated using Bayesian inference with uninformative priors. The joint log-likelihood function ℓ is derived in Appendix 3 (Eq. 13). We used a random walk Metropolis algorithm to sample from ℓ using the function MCMCmetrop1R of the R-package MCMCpack. Proposal samples for β were drawn from a Gaussian jumping distribution without cross-correlation between the parameters. In order to achieve a well-mixed chain the jumping variances were manually adjusted to achieve a Metropolis acceptance rate of around 0.5, while keeping the degree of autocorrelation between subsequent samples similar for each parameter. We used 10^5 burn-in samples per chain. After this burn-in the chains had converged, as tested by Gelman and Rubin's (1992) convergence diagnostic on two parallel chains with different starting values. On a converged chain we took 2000 samples for estimating the variance–covariance matrix of the model parameters β.

Model comparison

To make pairwise comparisons of model performance we compared joint log-likelihood values using Vuong's

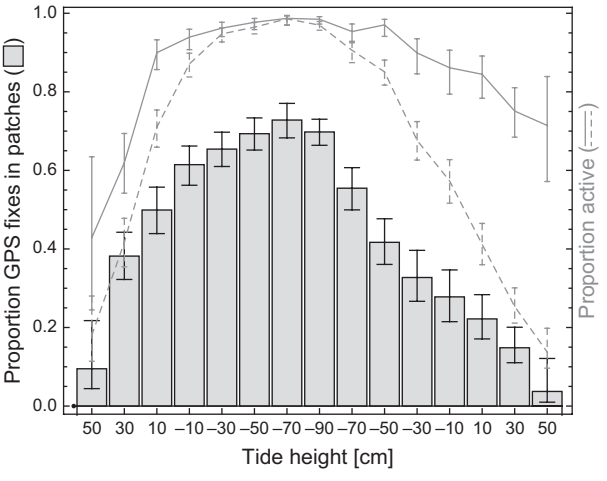

Figure 2. Bars indicate the proportion of GPS fixes occurring in the sampled grids for the period 2011-10-15 to 2011-11-15 (bars/left axis), as a function of tide height measured at a reference location (blue cross in Fig. 1). The proportion of oystercatchers active (dotted grey line) and the proportion active inside sampled grids (solid grey line) has been determined from accelerometer data. We calculated binomial proportion confidence intervals using the Wilson score interval, at a confidence level of 95%.

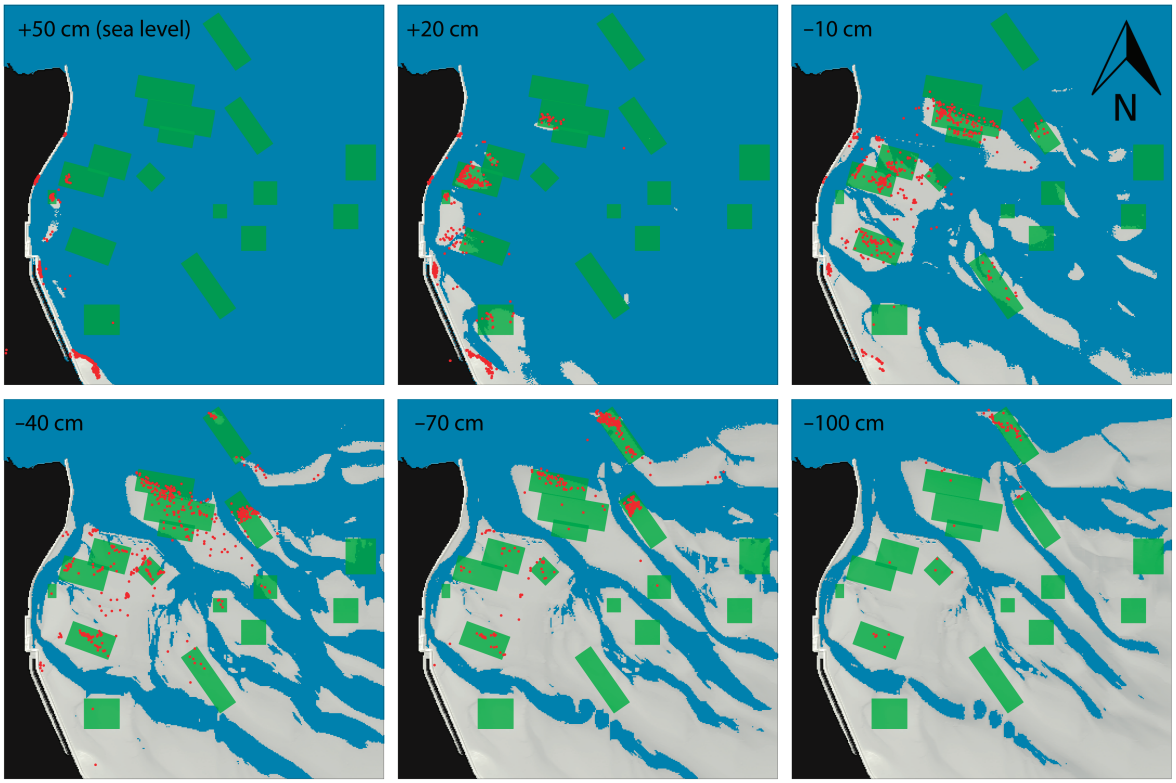

Figure 3. Oystercatcher GPS positions (red dots) of 10 individuals in the period 2011-10-15 to 2011-11-15 split out in panels by tidal height (at the time and position of each GPS fix) during falling tide. Blue indicates areas where the bathymetric height is below the indicated tidal height at each panel. Birds associate with the tide line and have a preference for the northerly deeper tidal zone, rich in *Ensis directus* prey.

likelihood ratio test for non-nested models (Vuong 1989) available in the spatcounts package. This likelihood ratio test is specifically designed to compare models of very different structure, complexity and parameter numbers, as applies to our behaviour-based models. Before applying the test, the model likelihoods were adjusted by the Schwarz correction (Burnham and Anderson 2002) as in BIC, to penalise models with a higher number of free parameters.

Data deposition

Data available from the Dryad Digital Repository: <http://dx.doi.org/10.5061/dryad.s8n05> (Dokter et al. 2017).

Results

Food landscape and dynamic foraging distribution

Since the spatial distribution of food critically determines the distribution patterns of oystercatchers, we first describe the results of the benthic survey of the food stock. The staple food of oystercatcher included adult cockles (Fig. 1, indicated in orange) and spat of the razor clam *Ensis directus* (Fig. 1, indicated in blue), the latter found only in deeper patches in the north of the study site (Dekker and Beukema 2012). Figure 1 reveals a prominent fine-scale structuring of the benthic resources, as further evidenced by a short variogram range for cockle numerical density (150 m, using a spherical variogram model, Supplementary material Fig. A8). The variogram range for cockle size was much larger (420 m), suggesting that over larger areas cockles dated from the same spat fall and were of similar age. The adult cockle size was 35 ± 4 mm ($n = 3014$, mean $\pm$ SD).

The change in number of oystercatchers on the sampled mudflats is illustrated in Fig. 2, showing the proportion of oystercatchers (bars) and their accelerometer-derived activity (solid line) in the sampled grids, as well as their overall activity (dashed line, inside and outside the sampled grids combined). The figure shows that during high tide birds were mostly resting, but when present in the grids they were highly active (> 80% of the time), indicative of foraging behaviour (Shamoun-Baranes et al. 2012). We may therefore assume that the GPS fixes inside the sampled grids are primarily associated with actively foraging oystercatchers, which can thus be modelled as foraging distributions. Figure 1 shows how 10 individually tracked oystercatchers distributed over the resource landscape, showing one month of location data during falling tide, split out in panels by tidal stage. Several qualitative features are noteworthy. First, many oystercatcher positions occur relatively close to the tide line, suggesting the birds are continuously adjusting their position in response to the retreating water. Second, in the low tidal stages most oystercatcher positions are found in the deepest patches containing razor clam spat (indicated in blue in Fig. 1). Intake rates were estimated by applying functional responses to the maps of prey size and numerical density. In the patches with razor clams intake rates were up to 1.0 mg AFDM s^{-1}, which

Table 1. Comparison of foraging distribution models, based on GPS telemetry data of oystercatchers collected in the period 15 October–15 November (sample size 10 individuals, in total M = 2876 GPS observations in the sampled grids) and the reconstructed food landscape. Subscripts j indicate dependence on prey type (cockle or clam). f = capture rate, G = prey response, b = energetic content of the prey item, K = damage costs, I = density-dependence/interference, I_0 = density dependence of intake-rates only. D indicates the deviance, i.e. $-2\Delta\ell$ with $\Delta\ell$ the difference in maximum joint log-likelihood with the model with the best fit (model 1, $\ell = -22242$). n gives the number of free parameters in the model. BIC (Bayesian information criterion) penalises the number of model parameters according to $-2\Delta\ell + n\log(M)$, with ΔBIC the difference in BIC relative to model with lowest BIC (model 2). V indicates pairwise significant differences in BIC according to Vuong's non-nested test at 95% confidence level. Model pairs labeled by different letters refer to significant differences. The test shows model 1 and 2 are the two most parsimonious models, with equivalent BIC values. The total number of birds in the system equalled n = 5000, with a proportion released on the foraging patches depending on the tidal phase (Fig. 2).

Model	Description	Gain rate formula	D	n	ΔBIC	V
1	full model	$f_j \times G_j \times b_j \times K_j \times I_j$	0	8	2	a
2	no prey-variation in prey response	$f_j \times G \times b_j \times K_j \times I_j$	14	6	0	a
3	no prey response	$f_j \times b_j \times K_j \times I_j$	110	4	80	b
4	no prey-var. in density-dependence	$f_j \times G_j \times b_j \times K_j \times I$	168	7	162	b
5	digestive intake rate	$f_j^{digest} \times G_j \times b_j \times K_j \times I_j$	332	8	334	c
6	no damage costs	$f_j \times G_j \times b_j \times I_j$	402	7	396	d
random	evenly over exposed patches	1	3588	0	3526	e
null	maximised intake rate	$f_j \times b_j \times I_0$	3588	2	3542	e

is considerably lower than in the patches with cockles, where oystercatchers reached up to 2.4 mg AFDM s^{-1}. Resampling the food landscape in the next spring revealed all razor clam beds were fully depleted over the winter, while cockle beds were not.

Ranking distributional mechanisms

To determine which mechanisms explain the observed distribution patterns, six behaviour-based models of different structural complexity were tested, as listed in Table 1. The gain rate formula indicates which model components, as introduced in methods section, were included. All model parameters are listed in Table 2. Parameter estimates by Bayesian MCMC methods are listed in Table 3.

We first tested the hypothesis of intake rate maximisation, which may be considered the traditional IFD null model. We assumed the value of the interference constant q_{cockle} corresponded to the reduction in intake rate with conspecific density, as found for oystercatchers foraging on cockles. We added the constraint that interference on razor clams should be weaker than the value for cockles, otherwise leaving q_{clam} a free model parameter. We find that such an IFD model of intake rate maximising birds (model 'null') cannot describe the observational data. The model does not perform better than a model in which birds are distributed evenly over the available patches (model 'random').

It is clear that additional foraging mechanisms strongly affected the observed distribution patterns, which we explored by including additional mechanistic components to account for damage costs (term K_j), an active prey effect (term G_j), and by leaving both interference parameters (term I_j) to be optimised freely. Predictions of this full model, after Bayesian estimation of its free parameters, are shown in Fig. 4. To quantify the contribution of its mechanistic components, we calculated the loss in BIC model performance when a mechanistic component was removed (Table 1, model 2–6). Removal of certain model components

Table 2. Overview of model parameters and their source. First column refers to the numbering of model components in methods. †cockle size s in units of mm. §Polynomial re-fit on intake rate data of a compilation of 10 studies, given in Zwarts et al. (1996, Fig. 16). ‡Value taken for oystercatchers feeding on *Macoma balthica*. *Values for October/November 2011, long-term benthos monitoring programme Balgzand, in Supplementary material section 4.

Comp.	Parameter	Symbol	Value	Unit	Source
1	attack rate cockle	A_{cockle}	0.000860	$m^{-2}\ s^{-1}$	Zwarts et al. 1996§
1	attack rate clam	A_{clam}	0.000625	$m^{-2}\ s^{-1}$	Hiddink 2003‡
1	handling time cockle	h_{cockle}	$0.2205s^{1.7921}$†	s	Zwarts et al. 1996§
1	handling time clam	h_{clam}	13.4	s	suppl. 5.2, this study
1	digestion rate shellfish	r_{digest}	0.7	$Mg\ s^{-1}$	Kersten and Visser 1996
2	prey response cockle	B_{cockle}	free	–	Eq. 3, this study
2	prey response clam	B_{clam}	free	–	Eq. 3, this study
2	decay prey resp. cockle	τ_{cockle}	free	h	Eq. 3, this study
2	decay prey resp. clam	τ_{clam}	free	h	Eq. 3, this study
2	mean low tide	$\bar{L}$	6.2	h	Eq. 4, this study
3	body mass index cockle	BMI_{cockle}	9	$mg\ cm^{-3}$	R. Dekker pers. comm.*
3	body mass index clam	BMI_{clam}	0.48	$mg\ cm^{-3}$	R. Dekker pers. comm.*
4	damage factor cockle	K_{cockle}	free	–	Eq. 6, this study
4	damage factor clam	K_{clam}	1	–	Eq. 6, this study
5	interference cockle	q_{cockle}	0.08 or free	10^{-2} ha	Rappoldt et al. 2010
5	interference clam	q_{clam}	free	10^{-2} ha	Eq. 7, this study
	random fraction	f_{random}	free	–	Eq. 14, this study

Table 3. Parameters for the models in Table 1 that were estimated on a combination of benthic survey data and tracking data (10 individual birds, M = 2876 gps observations in the sampled grids). Values in parenthesis are standard errors. * or ** indicates this model component was removed from the model by fixing the parameter value to 0 or 1, respectively. ‡f_{random} indicates the proportion of animals distributed randomly over the available area; Eq. 13 Appendix 2. †value calculated according to the relation $q = \pi\alpha D_A^2$, parametrised following the observational and modelling data of Stillman et al. (2002), i.e. $D_A = 3.3$ and $\alpha = 0.241$ (Rappoldt et al. 2010, Table 1).

		Damage K	Prey response G				Interference I	
Model	f_{random}‡	K_{cockle}	τ_{cockle} [h]	τ_{clam}[h]	B_{cockle}	B_{clam}	q_{cockle} [10^{-2} ha]	q_{clam} [10^{-2} ha]
1	0.28 (0.01)	0.17 (0.01)	0.07 (0.03)	0.04 (0.01)	1.8 (0.1)	0.6 (0.1)	16.2 (0.6)	1.70 (0.07)
2	0.33 (0.01)	0.17 (0.01)	0.02 (0.07)	τ_{cockle}	0.7 (0.1)	B_{cockle}	11.5 (0.4)	1.75 (0.05)
3	0.33 (0.01)	0.09 (0.01)	*	*	*	*	13 (1)	1.85 (0.07)
4	0.34 (0.00)	0.10 (0.00)	0.05 (0.01)	0.01 (0.01)	0.31 (0.08)	2.1 (0.2)	3.25 (0.06)	q_{cockle}
5	0.33 (0.01)	0.49 (0.01)	0.10 (0.01)	0.02 (0.01)	0.14 (0.03)	0.54 (0.06)	2.2 (0.1)	1.04 (0.03)
6	0.15 (0.00)	**	0.21 (0.03)	0.02 (0.01)	7.1 (0.1)	0.03 (0.02)	71 (1)	1.2 (0.1)
random	**	**	*	*	*	*	*	*
null	0.99 (0.00)	**	*	*	*	*	0.08†	0.04 (0.03)

came at a much higher performance loss than others, allowing a ranking of which mechanisms were the most important drivers of the distributional patterns.

The direct predator–prey effect of bill damage avoidance had the largest effect size in explaining foraging distributions (see model 6 'no damage costs' versus model 1 'full model'). The importance of intake rate selection was evaluated by a model in which interference-free intakes rate above the digestion rate r_{digest} were perceived as equivalent by the model birds, similar to a digestive rate model (van Gils and Piersma 2004). This removed most of the selectivity for intake rates, because around half of the patches in our system had an interference-free intake rate above r_{digest}. Selection for intake rates had the second largest effect size (see model 5 'digestive intake rate' versus model 1 'full model').

Compared to the former two direct predator–prey effects, the density-dependent effect of prey-differences in interference was considerably smaller (see model 4 'no variation in density-dependence' versus full model). For both prey types the magnitude of the exponential interference constants exceeded 1 ha, suggesting that density dependent regulation of bird distributions already played a role at densities of a few birds ha^{-1}. The optimised interference constants were higher for cockles than for razor clams (cf. Table 3).

There was also evidence for an active prey response (see model 3 'no prey response' versus full model), which was found to be very short-lived (less than 10 min, cf. Table 3). We found no evidence that the prey response varied with prey type, because model 2 'no prey variation in prey response' performed as well as the full model.

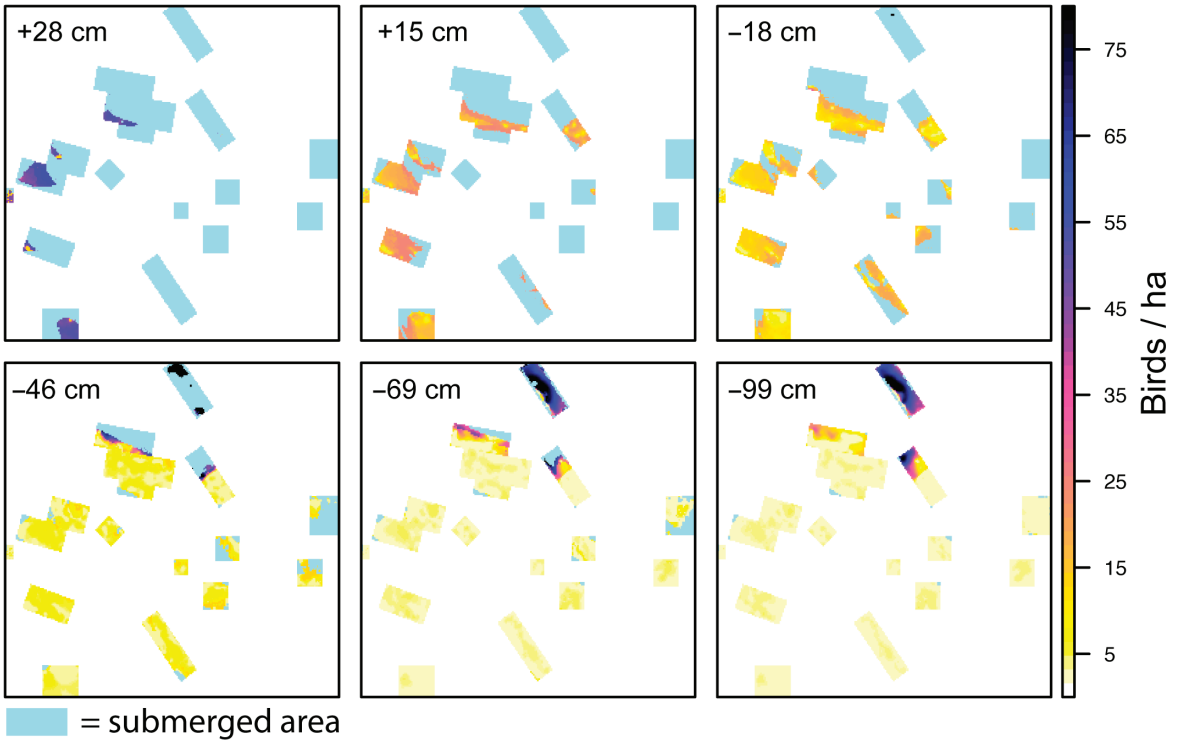

Figure 4. Predicted bird densities by model 1 on 2011-10-29 10:50, 11:10, 12:00, 12:50, 13:40, 15:10 UTC, corresponding to tidal heights at the reference point of 28, 15, -18, -46, -69, -99 cm MSL, respectively. For other models see Supplementary material section 6.

Discussion

Balance of density-dependent and density-independent mechanisms

According to our ranking of established foraging mechanisms of the oystercatcher (Table 1), spatial distributions were primarily explained by density-independent effects. Interference effects, and spatial variations in density dependence in general, played only a secondary role in explaining oystercatchers space use, in spite of oystercatchers being interference-prone and a model for competitive distributions.

Although landscape-scale distributions were dominated by density-independent interactions, this does not imply that conspecifics had no effect on each other. It is well established that short-range interactions can affect the finest inter-individual positions (Moody and Thompson 1997). Also, mortality rates of oystercatchers can become density-dependent in certain periods (Le V Dit Durell et al. 2000). In our case the razor clam beds became fully depleted over the winter, suggesting that competition through depletion may have played a role.

Importantly, however, although competitive interactions may affect foragers, in our density-dependent analysis these interactions turned out less important for explaining the aspect of landscape-scale distribution. Complex density-independent tradeoffs, such as the negotiation of energetic gains and body damage, were more of a bottleneck in our understanding of spatial distributions of this interference-prone species.

A striking feature of the better models is a high value of the optimised interference constants (cf. Table 3, up to 1620 m^2). These magnitudes suggest that density-dependent regulation operated over long distances already at low bird densities (by Eq. 7, gain rate decreased by a factor 1/e already at 6 birds ha^{-1}). Intake rates are known to decrease by interference only at densities above 50–100 birds ha^{-1} (Triplet et al. 1999), corresponding to much lower interference constants (5–12 m^2, cf. Stillman et al. 2002, Rappoldt et al. 2010, Rutten et al. 2010a). The high interference constants thus contradict our initial hypothesis that density-dependent regulation occurs primarily through short-range mutual interactions affecting intake, like conflicts over food.

Larger interference constants can be explained from birds pre-emptively avoiding each other over longer distances (Moody and Thompson 1997, Rutten et al. 2010a, Gyimesi et al. 2010), such that less notice of competitors is required. Avoidance also increases the chance of exploring regions where competitors have not yet depleted easily accessible prey items, and where prey is not yet depressed (Charnov et al. 1976).

When suitable prey is cryptic or hard to find, explorative behaviour is generally an important strategy to increase foraging success, and will spread out animals further compared to an IFD (van Gils 2010, Matsumura et al. 2010). The resultant increase in mean inter-individual distances may also have reduced effects of short-range mutual interactions on landscape-scale spatial distributions, and contributed to higher apparent interference constants, as both observed in this study.

The extent to which interference determines land-scape scale distributions always depends on the prey stock and the susceptibility to interference of available prey types. Especially when food is concentrated in small areas, forcing animals to forage closely together, it is conceivable that interference gains importance in regulating landscape-scale distributions. In the case of oystercatchers, this may apply to food lanscapes dominated by dense stable mussel beds with only small stocks of alternative foods, like in the estuary of the Exe, where kleptoparasitism was found to be common and mortality density-dependent (Ens and Goss-Custard 1984, Goss-Custard et al. 2001). Such sites will be particularly informative to further test the role of conspecific interference on the aspect of spatial distribution.

Density-dependent analysis of oystercatcher prey preferences

In this study we focussed on disentangling the relative contributions of well-established factors thought to be of overall importance to foraging oystercatchers. More subtle individual differences in dominance, bill condition or age were not accounted for, as this would require very high sample sizes of tracked individuals. Patterns in tracking data were similar between individuals, showing strong selection of razor clams during the lowest tides. This pattern was confirmed by supporting field observations, when thousands of birds were observed foraging on the razor clam beds as soon as these deep areas were exposed. These observations support our assumption that the cohort of tracked individuals sampled the population-average foraging behaviour.

Our model analysis showed preference for razor clams over cockles, which may involve both density-dependent and density-independent responses to this prey. The preference could not be explained from considerations of intake rates, because intake rates on razor clams were relatively low, and higher intake rates could be realised on cockles. It could neither be explained from a relatively high capture probability of clams directly after exposure. Tracking data showed that foraging oystercatchers were often found close to the tide line, indicating a high prey availability at the tide line, which gave rise to a significant prey response G. Birds thus exploited a temporary window of opportunity directly after exposure (possibly prey quickly takes protective measures to avoid predation, such that prey availability decreases after exposure). However, we found no evidence that this active prey effect differed between prey types, and it therefore could not explain differences in preference for razor clams versus cockles.

This leaves interference I_j, accounting for prey differences that were density-dependent, and damage costs K_j, accounting for prey differences that were density-independent. Cockles are difficult to open (Rutten et al. 2006) but have a high flesh content (Zwarts et al. 1996). Because of a long handling time, foraging on cockles is sensitive to interference by kleptoparasitism. This is different for the razor clam spat, which are buried vertically into the top layer of the sediment. Spat cannot hide very deeply in the sediment yet (like adult razor clams), and remain accessible to oystercatchers. Since their shells are thin and do not close at the top, they can be easily and quickly captured and consumed (Dekker and

Beukema 2012, Freudendahl et al. 2010). Foragers on this prey are therefore expected to be less susceptible to interference. Indeed we found evidence for a stronger interference effect on cockles than on razor clams (cf. Table 3). However, the additional model performance resulting from prey-specific density-dependence was considerably smaller than that from damage cost avoidance, a density-independent model component. Razor clam preference should therefore primarily be explained from easy capture without risk of bill damage, a density-independent effect, and not from a lower susceptibility to interference. This result again points to a stronger contribution of density-independent effects relative to density-dependent effects in determining habitat choice.

The effects of damage cost avoidance were likely relatively strong in our study year, because the cockle cohort was at the upper range of the preferred size class by oystercatchers (Sutherland 1982). Only when cockles are large, oystercatchers have a substantial risk of bill damage when opening the shells (Rutten et al. 2006), and in years with smaller cockles this prey may be selected more.

Effects of bill damage in relation to cockle size are generally missing in conventional IFD models based on generalised functional responses. Damage cost avoidance is also not included in the two contemporary models that are currently being used to assess the effects of environmental change and fisheries for this species (MORPH, Stillman et al. 2000, and WEBTICS, Rappoldt et al. 2004). Careful consideration of the true food stock requirements of foragers and their dynamic distributions will be essential to make such assessments realistic and reliable.

Behaviour-based modelling of tracking data in a Bayesian framework

Studies quantifying the relative contribution of density-dependent versus density-independent interactions to landscape-scale foraging patterns of free-living birds are still extremely rare (McLoughlin et al. 2010). We hope this study will be useful as a roadmap for other density-dependent analyses of tracking data, which are needed to test the generality of our findings across a wider range of periods and species.

The critical modelling step in this study was casting a (density-dependent) optimality model (Eq. 1) into a likelihood function (Eq. 13) that connects the model to tracking data observations. This allowed us to rank model performance and estimate free parameters (and their uncertainties and correlations) using standard Bayesian statistics. Because this approach generalises to patterns and models that are dynamic and spatially complex, it is especially suited for making inferences from information-rich patterns of individual tracking data.

Patterns both at the fine scales (e.g. data underlying functional responses) and larger scales (e.g. patterns in tracking data and benthos surveys) were considered simultaneously when parametrising and comparing candidate models. Such a hierarchical approach combining multiple scales has also been advocated in pattern-oriented modelling (POM), in order to make models more realistic and predictive (Grimm and Railsback 2012). However, where POM strictly separates the steps of model selection, parametrisation and calibration (Grimm and Railsback 2012), we used (Bayesian) information theoretic techniques, in which model comparison and parametrisation are intimately linked (Burnham and Anderson 2002).

The advantage of a Bayesian approach is that uncertainty and prior knowledge on model parameters can be incorporated in a natural way as priors, or parameter values with high uncertainties can be left unspecified when comparing candidate models. In the case of oystercatchers, bill injury avoidance, tidal changes in prey availability and conspecific interference are processes that are difficult to accurately parametrise beforehand on the basis of available literature or independent experiments (van der Meer and Ens 1997, Rutten et al. 2006, 2010a), which is why these parameters were freely optimized on the tracking data. Subsequent model comparisons were therefore less dependent of subjective (and possibly inaccurate) a priori parametrisations, by which we aimed to steer comparisons towards the candidate mechanisms the models represent, which are of primary interest.

Acknowledgments – We thank Landschap Noord-Holland for providing monthly oystercatcher counts, and Rob Dekker for providing BMI data of benthos of the Balgzand area.
Funding – This research was partly funded through the project 'Monitoring abundance, composition, development and spatial variation in macrozoobenthos and birds' of the national programme for sea and coastal research (ZKO) of the Netherlands Organization for Scientific Research (NWO). NAM funded the GPS-trackers. Our bird behavioural studies are supported by the UvA-BiTS virtual lab on the Dutch national e-infrastructure, built with support of LifeWatch, the Netherlands eScience Center, SURFsara and SURFfoundation.

References

Bartlam-Brooks et al. 2013. In search of greener pastures: using satellite images to predict the effects of environmental change on zebra migration. – J. Geophys. Res. Biogeosci. 118: 1427–1437.

Bautista, L. M. et al. 1995. A field test of ideal free distribution in flock-feeding common cranes. – J. Anim. Ecol. 64: 747–757.

Beukema, J. J. 1974. seasonal changes in the biomass of the macro-benthos of a tidal flat area in the dutch wadden sea. – Neth. J. Sea Res. 8: 94–107.

Beukema, J. J. and Cadée, G. C. 1997. Local differences in macrozoobenthic response to enhanced food supply caused by mild eutrophication in a Wadden Sea area: food is only locally a limiting factor. – Limnol. Oceanogr. 42: 1424–1435.

Bouten, W. et al. 2013. A flexible GPS tracking system for studying bird behaviour at multiple scales. – J. Ornithol. 154: 571–580.

Brown, J. S. and Kotler, B. P. 2004. Hazardous duty pay and the foraging cost of predation. – Ecol. Lett. 7: 999–1014.

Burnham, K. and Anderson, D. 2002. Model selection and multimodel inference: a practical information-theoretic approach, 2nd edn. – Springer.

Charnov, E. L. et al. 1976. Ecological implications of resource depression. – Am. Nat. 110: 247–259.

Dekker, R. and Beukema, J. J. 2012. Long-term dynamics and productivity of a successful invader: the first three decades of the bivalve *Ensis directus* in the western Wadden Sea. – J. Sea Res. 71: 31–40.

Dokter, A. et al. 2017. Data from: Balancing food and density-dependence in the spatial distribution of an interference-prone forager. – Dryad Digital Repository, <http://dx.doi.org/10.5061/dryad.s8n05>.
Duijns, S. and Piersma, T. 2014. Interference competition in a sexually dimorphic shorebird: prey behaviour explains intraspecific competition. – Anim. Behav. 92: 195–201.
Duijns, S. et al. 2015. Field measurements give biased estimates of functional response parameters, but help explain foraging distributions. – J. Anim. Ecol. 84: 565–575.
Elias, E. and Wang, Z. B. 2013. Abiotische gegevens voor monitoring effect bodemdaling. – Deltares, Delft.
Ens, B. J. and Goss-Custard, J. D. 1984. Interference among oystercatchers, *Haematopus ostralegus*, feeding on mussels, *Mytilus edulis*, on the Exe Estuary. – J. Anim. Ecol. 53: 217–231.
Folmer, E. O. et al. 2012. The spatial distribution of flocking foragers: disentangling the effects of food availability, interference and conspecific attraction by means of spatial autoregressive modeling. – Oikos 121: 551–561.
Fretwell, S. D. and Lucas, H. L. 1969. On territorial behavior and other factors influencing habitat distribution in birds. I. Theoretical developments. – Acta Biotheor. 19: 16–36.
Freudendahl, A. S. L. et al. 2010. The introduced clam *Ensis americanus* in the Wadden Sea: field experiment on impact of bird predation and tidal level on survival and growth. – Helgoland Mar. Res. 64: 93–100.
Galassi, M. et al. 2009. GNU Scientific library reference manual, 3rd edn. – Network Theory Ltd.
Gelman, A. and Rubin, D.B. 1992. Inference from iterative simulation using multiple sequences. – Stat. Sci. 7: 457–511.
Goss-Custard, J. D. et al. 1995. Deriving population parameters from individual variations in foraging behaviour. I: Empirical game theory distribution model of oystercatchers *Haematopus ostralegus* feeding on mussels *Mytilus edulis*. – J. Anim. Ecol. 64: 265–276.
Goss-Custard, J. D. et al. 2001. Density-dependent starvation in a vertebrate without significant depletion. – J. Anim. Ecol. 70: 955–965.
Graveland, J. and Berends, A. E. 1997. Timing of the calcium intake and effect of calcium deficiency on behaviour and egg laying in captive great tits, *Parus major*. – Physiol. Zool. 70: 74–84.
Grimm, V. and Railsback, S. F. 2012. Pattern-oriented modelling: a 'multi-scope' for predictive systems ecology. – Phil. Trans. R. Soc. B 367: 298–310.
Gyimesi, A. et al. 2010. Cryptic interference competition in swans foraging on cryptic prey. – Anim. Behav. 80: 791–797.
Hiddink, J. G. 2003. Modelling the adaptive value of intertidal migration and nursery use in the bivalve *Macoma balthica*. – Mar. Ecol. Prog. Ser. 252: 173–185.
Holling, C. S. 1959. Some characteristics of simple types of predation and parasitism. – Can. Entomol. 91: 385–398.
Honkoop, P. J. C. and Beukema, J. J. 1997. Loss of body mass in winter in three intertidal bivalve species: an experimental and observational study of the interacting effects between water temperature, feeding time and feeding behavior. – J. Exp. Mar. Biol. Ecol. 212: 277–297.
Hornman, M. et al. 2013. Watervogels in Nederland in 2010/2011. – Sovon Vogelonderzoek Nederland, Nijmegen.
Houston, A. I. and McNamara, J. M. 2014. Foraging currencies, metabolism and behavioural routines. – J. Anim. Ecol. 83: 30–40.
Hulscher, J. B. 1982. The oystercatcher *Haematopus ostralegus* as a predator of the bivalve *Macoma balthica* in the Dutch Wadden Sea. – Ardea 70: 89–152.
Kacelnik, A. et al. 1992. The ideal free distribution and predator–prey populations. – Trends Ecol. Evol. 7: 50–55.
Kennedy, M. and Gray, R. D. 1993. Can ecological theory predict the distribution of foraging animals? A critical analysis of experiments on the ideal free distribution. – Oikos 68: 158–166.
Kersten, M. and Visser, W. 1996. The rate of food processing in the oystercatcher: food intake and energy expenditure constrained by a digestive bottleneck. – Funct. Ecol. 10: 440–448.
Le V Dit Durell, S. E. A. et al. 2000. Density-dependent mortality in oystercatchers *Haematopus ostralegus*. – Ibis 142: 132–138.
Lessells, C. M. 1995. Putting resource dynamics into continuous input ideal free distribution models. – Anim. Behav. 49: 487–494.
Manly, B. F. J. et al. 2002. Resource selection by animals: statistical design and analysis for field studies, 2nd edn. – Springer.
Martínez, I. et al. 2011. Disentangling the formation of contrasting tree-line physiognomies combining model selection and Bayesian parameterization for simulation models. – Am. Nat. 177: E136–52.
Matsumura, S. et al. 2010. Foraging on spatially distributed resources with sub-optimal movement, imperfect information, and travelling costs: departures from the ideal free distribution. – Oikos 119: 1469–1483.
Matthiopoulos, J. et al. 2011. Generalized functional responses for species distributions. – Ecology 92: 583–589.
McLoughlin, P. D. et al. 2010. Considering ecological dynamics in resource selection functions. – J. Anim. Ecol. 79: 4–12.
Milinski, M. 1994. Ideal free theory predicts more than only input matching: a critique of Kennedy and Gray's review. – Oikos 71: 163–166.
Moody, A. L. and Thompson, W. A. 1997. The analysis of the spacing of animals, with an example based on oystercatchers during the tidal cycle. – J. Anim. Ecol. 66: 615–628.
Mysterud, A. and Ims, R. A. 1998. Functional responses in habitat use: availability influences relative use in tradeoff situations. – Ecology 79: 1435–1441.
Oudman, T. et al. 2014. Digestive capacity and toxicity cause mixed diets in red knots that maximize energy intake rate. – Am. Nat. 183: 650–659.
Pebesma, E. J. 2004. Multivariable geostatistics in S: the gstat package. – Comput. Geosci. 30: 683–691.
Quaintenne, G. et al. 2011. Scaling up ideals to freedom: are densities of red knots across western Europe consistent with ideal free distribution? – Proc. R. Soc. B 278: 2728–2736.
Rappoldt, C. et al. 2004. Wader energy balance and tidal cycle simulator WEBTICS. – Alterra, Wageningen.
Rappoldt, C. et al. 2010. A geometrical model for the effect of interference on food intake. – Ecol. Model. 221: 147–151.
Recher, H. F. 1966. Some aspects of the ecology of migrant shorebirds. – Ecology 47: 393–406.
Rutten, A. L. et al. 2006. Optimal foraging on perilous prey: risk of bill damage reduces optimal prey size in oystercatchers. – Behav. Ecol. 17: 297–302.
Rutten, A. L. et al. 2010a. Experimental evidence for interference competition in oystercatchers, *Haematopus ostralegus*. I. Captive birds. – Behav. Ecol. 21: 1251–1260.
Rutten, A. L. et al. 2010b. Experimental evidence for interference competition in oystercatchers, *Haematopus ostralegus*. II. free-living birds. – Behav. Ecol. 21(6): 1261–1270.
Schwemmer, P. et al. 2016. Modelling small-scale foraging habitat use in Eurasian oystercatchers (*Haematopus ostralegus*) in relation to prey distribution and environmental predictors. – Ecol. Model. 320: 322–333.
Shamoun-Baranes, J. et al. 2012. From sensor data to animal behaviour: an oystercatcher example. – PLoS ONE 7(5): e37997.
Stillman, R. A. et al. 2000. Predator search pattern and the strength of interference through prey depression. – Behav. Ecol. 11: 597–605.
Stillman, R. A. et al. 2002. Predicting the strength of interference more quickly using behaviour-based models. – J. Anim. Ecol. 71: 532–541.

Sutherland, W. J. 1982. Do oystercatchers select the most profitable cockles? – Anim. Behav. 30: 857–861.
Sutherland, W. J. 1983. Aggregation and the 'ideal free' distribution. – J. Anim. Ecol. 52: 821–828.
Tregenza, T. 1995. Building on the ideal free distribution. – Adv. Ecol. Res. 26: 253–302.
Triplet, P. et al. 1999. Prey abundance and the strength of interference in a foraging shorebird. – J. Anim. Ecol. 68: 254–265.
Turner, M. G. 1989. Landscape ecology: the effect of pattern on process. – Annu. Rev. Ecol. Syst. 20: 171–197.
van de Pol, M. et al. 2014. A global assessment of the conservation status of the nominate subspecies of Eurasian oystercatcher *Haematopus ostralegus ostralegus*. – Int. Wader Studies 20: 47–61.
van der Meer, J. and Ens, B. J. 1997. Models of interference and their consequences for the spatial distribution of ideal and free predators. – J. Anim. Ecol. 66: 846–858.
van Gils, J. A. 2010. State-dependent Bayesian foraging on spatially autocorrelated food distributions. – Oikos 119: 237–244.
van Gils, J. A. and Piersma, T. 2004. Digestively constrained predators evade the cost of interference competition. – J. Anim. Ecol. 73: 386–398.
van Gils, J. A. et al. 2004. Carrying capacity models should not use fixed prey density thresholds: a plea for using more tools of behavioural ecology. – Oikos 104: 197–204.
van Gils, J. A. et al. 2005. Digestive bottleneck affects foraging decisions in red knots *Calidris canutus*. I. Prey choice. – J. Anim. Ecol. 74: 105–119.
van Gils, J. A. et al. 2006. Foraging in a tidally structured environment by red knots (*Calidris canutus*): ideal, but not free. – Ecology 87: 1189–1202.
Vuong, Q. H. 1989. Likelihood ratio tests for model selection and non-nested hypotheses. – Econometrica 57: 307–333.
Wood, K. A. et al. 2013. Go with the flow: water velocity regulates herbivore foraging decisions in river catchments. – Oikos 122: 1720–1729.
Zwarts, L. et al. 1996. Causes of variation in prey profitability and its consequences for the intake rate of the oystercatcher *Haematopus ostralegus*. – Ardea 84A: 229–268.

Supplementary material (available online as Appendix oik-04139 at <www.oikosjournal.org/appendix/oik-04139>). Balancing food and density-dependence in the spatial distribution of an interference-prone forager.

Appendix 1. Expressing K_j into a damage rate

To account for the negative effects of body damage, we need a common currency by which we may titrate between such costs of body damage and the benefits of food intake (Brown and Kotler 2004). Following Houston and McNamara (2014) we define V(x,y) to be the expected future lifetime reproductive success of an animal with energy reserves x and condition y (of body or bill). The rate at which the animal increases energy reserves x is given by the capture rate times b_j. Let us further assume that condition y is lost at a rate $\kappa_j(s)$ when foraging on prey type j of size s as a result of damage. If we assume bill damage only occurs while handling prey, which takes a time $h_j(s)$ for a prey item of type j and size s, the energetic gain per prey item including the cost of damage $\widetilde{b_j}$ can be written as

$$\widetilde{b_j}(s)=b_j(s)K_j(s), K_j(s)=1-\kappa_j(s)\frac{h_j(s)}{b_j(s)}\frac{\partial V/\partial y}{\partial V/\partial x} \quad (8)$$

$$\widetilde{b_j}(s)=b_j(s)-\kappa_j(s)h_j(s)\frac{\partial V/\partial y}{\partial V/\partial x} \quad (9)$$

Here the term $(\partial V/\partial y)/(\partial V/\partial x)$ is the marginal rate of substitution of the value of condition to the value of energy (Houston and McNamara 2014). Because the cost of damage for foraging on razor clam spat is negligible compared to the cost of damage for foraging on cockles, we may set $\kappa_{clam} = 0$ (i.e. $K_{clam}(s) = 1$). $K_{cockle}(s) = K_{cockle}$ we retain as the only model parameter. Because the handling time $h_{cockle}(s)$ is approximately proportional to s^2 (Zwarts et al. 1996) and the biomass $b_{cockle}(s)$ to s^3, a parameter K_{cockle} independent of s amounts to the assumption that the damage rate $\kappa_{cockle}(s)$ is proportional to cockle size s, such that larger cockles inflict more damage.

Appendix 2. Solution of the IFD model

We define the interference-free gain rate in patch k at time t as $F_{kt} = f_j \times G_j \times b_j \times K_j$. Equation 1 and 7 may be rearranged to obtain the bird density at patch k at time t, also known as the numerical or aggregative response:

$$p_k(t,\beta)=p_k(t|q,\tau,B)=\begin{cases}\log(F_{kt}/c_t)/q, & F_{kt}>c_t\\ 0, & F_{kt}<c_t\end{cases} \quad (10)$$

where we defined $\beta = [q,\tau,B]$ the vector of parameters of the ideal-free model (in this example a model with three free parameters, assuming parameters for interference and prey effect do not differ between prey types). The maximised gain rate c_t is found by requiring that the sum over the available patches of bird density p_k times patch area a_k equals the total number of birds N_t in the system, which by Eq. 10 amounts to the boundary condition

$$\sum_{\substack{k\in S_t\\ F_{kt}>c_t}}\frac{a_k\log(F_{kt}/c_t)}{qN_t}=1 \quad (11)$$

where S_t is the set of exposed patches available to the animal at time t (the foragers' choice set, Manly et al. 2002). This solution to the IFD contains the interference constant q and the total number of birds N as multiplicative pairs. This implies that the (normalised) foraging distribution will be invariant to the total number of birds in the system, when

the interference constant is optimised as a free model parameter: doubling the number of model birds will simply produce an optimised interference constant that is twice as low, resulting in a model with the same proportional distribution and likelihood. This is a very useful property when the absolute number of birds in a limited study area is difficult to assess.

Solving the IFD given a parameter vector β involves finding the maximised gain rate c_t, which was implemented in a C module callable from R (<www.r-project.org>) using Brent's root finding method (Galassi et al. 2009).

Appendix 3. Likelihood of an IFD model given a set of location observations

To assess how well an IFD model describes distributional patterns obtained with individual tracking, we need to compare

- A set of animal location observations i (GPS fixes), each characterised by a location or selected patch k_i and a time t_i.
- A candidate animal distribution model $p_k(t|\beta)$, which predicts in each patch k of the system at any time t the animal density, conditional on its vector of model parameters β and the total number of animals N_t.

Quantitatively comparing these patterns becomes challenging especially when patterns are spatially complex and dynamic. Starting from the simple idea that the probability that a GPS location i is recorded in a patch k_i, should be directly proportional to forager density and size of that patch, we can write:

$$\ell_i = \frac{a_{k_i}}{N_{ti}} p_{ki}(t_i|\beta) \propto \text{probability of finding GPS fix i in patch } k_i \text{ at time } t_i \quad (12)$$

with ℓ_i the proportion of animals in patch k_i at time t_i, a_{k_i} the area of the patch and N_{t_i} the total number of animals in the system at time t_i. If the distribution model closely approximates reality, we expect most GPS fixes are found in patches with a high ℓ_i, that is, a good model maximises the overall ℓ_i values. Along these lines we can formulate a joint likelihood function that gives the overall likelihood of a model for the full set of M location observations, by multiplying the individual likelihoods ℓ_i of the GPS fixes. Taking the logarithm of this function gives us the joint log-likelihood function:

$$\ell(\beta) = \log \prod_{i=1}^{M} w_i \ell_i = \sum_{i=1}^{M} \log w_i \left[\frac{a_i}{N_{t_i}} \left(p_i(t_i|\beta) + p_0 \right) \right] \quad (13)$$

Here w_i is a weighting of GPS fixes for balancing sampling (we require $\Sigma_i w_i = M$). We require that sampling is balanced over all tidal stages (i.e. sea level heights encountered during both falling and rising tide), which is realised by inversely weighing each fix with the proportion of oystercatchers present in the system at the corresponding tidal stage (as given by the bars in Fig. 2). In this equation we also included an offset bird density p_0, given by:

$$p_0 = f_{random} N_{t_i} / \sum_{k \in S_{t_i}} a_k \quad (14)$$

S_{t_i} equals the set of exposed available patches available to the animal at time t_i. f_{random} is the proportion of animals which is distributed uniformly over the available area. This value represents the fraction of animals that is not actively foraging or that is unassociated with the food landscape, and at the same time prevents the model log-likelihood to become $-\infty$ (which would happen in an IFD model when GPS fixes occur in patches without resources).

This joint log-likelihood provides a metric to rank models according to the accuracy by which observed animal locations are predicted, i.e. it applies multi-model inference to the realm of behaviour-based modelling of tracking data, an approach that has rarely been taken so far (but see Martínez et al. 2011, Bartlam-Brooks et al. 2013). To compute Eq. 13 for a given β, we determined for each time t_i of each GPS fix i which grid points were exposed (and since when), and which proportion of birds was present in the system (following Fig. 2). This information, together with the spatial prey maps, was fed into the routines calculating a bird distribution for each time t_i according to Eq. 10. From these predicted distributions we obtained the predicted bird density at the location of each GPS fix, $p_i(t_i|\beta)$. These values were combined into a single joint log-likelihood value using Eq. 13. To calculate one joint log-likelihood value for a parameter vector β on the basis of M GPS fixes, we thus need to numerically solve M bird distributions (one at the instant of each GPS fix), which makes these calculations computationally expensive.